Earth Planets Space, **64**, 991–1003, 2012

Source mechanism of the 23 October, 2011, Van (Turkey) earthquake ($M_w = 7.1$) and aftershocks with its tectonic implications

T. Serkan Irmak[1], Bülent Dogan[2], and Ahmet Karakaş[2]

[1]*Kocaeli University, Department of Geophysical Engineering, Seismology Section, 41040, Kocaeli, Turkey*
[2]*Kocaeli University, Department of Geological Engineering, 41040, Kocaeli, Turkey*

(Received December 19, 2011; Revised April 18, 2012; Accepted May 5, 2012; Online published November 26, 2012)

This study has investigated the rupture process of the 23 October, 2011, Van (Turkey) earthquake ($M_w = 7.1$) by using inversion of teleseismic waveform analysis and its tectonic implications. Focal parameters of the main shock and 21 aftershocks were obtained by using the first motion polarities of regional P-waves. The first results for the source rupture process were derived from broadband teleseismic P-waves. The main outcomes of the analysis are: (a) the main rupture is located around the initial break point, and the maximum slip amount was 3.6 m; (b) the size of the main fault plane area was about 40 km in length and 20 km in width, the duration of rupture was approximately 19 seconds and the seismic moment of the earthquake was estimated to be 5.53×10^{19} N m ($M_w = 7.1$); (c) the rupture gradually expanded near the hypocenter and propagated both northeast and southwest, but mainly to the southwest. Tectonic implications of the earthquake were defined by field observations. The 23 October, 2011, Van earthquake occurred on a main thrust fault plane trending NE-SW between Lake Van and Lake Erçek located in the East Anatolian compressional province. This main fault plane and the secondary structural elements were generated by a continental-continental collision taking place in a region located 200 km north of the the Bitlis-Zagros Suture Zone.

Key words: Source rupture process, East Anatolian compressional province, Van earthquake, thrust fault, focal parameters.

1. Introduction

A destructive earthquake occurred on 23 October, 2011, at 10:41 (UTC) in Van, located in the east of Turkey (Fig. 1). The hypocenter determined by the Kandilli Observatory and Earthquake Research Institute (KOERI) is located at 38.7578N, 43.3602E, with a 15-km depth (KOERI, 2011). A total of 604 people were killed and more than 2500 people were injured, mainly by the collapse of buildings. A detailed earthquake report has been published by the Disaster and Emergency Management Presidency of Prime Ministry of Republic of Turkey (DEMP, 2011).

The tectonic setting of Turkey and east Anatolia is the main factor in earthquake occurrence. The movement of the Arabia plate towards the Eurasia plate occurring along the Bitlis-Zagros Suture Zone (BZSZ) has been continuing from Serravalien (∼12 Ma) to the present (Fig. 1(a)). This time interval is called the Neotectonic period for the East Anatolia region (Şengör and Y lmaz, 1981; Dewey *et al*., 1986; Koçyigit *et al*., 2001). The movement rate of the Arabia plate towards the Eurasia plate is about 20–30 mm/year according to GPS measurements (Reilinger *et al*., 2006). The effects of the continental-continental collision in East Anatolia prolongs to the north of the BZSZ, as E-W slicing thrusts (Şaroglu and Y lmaz, 1986). The collision created by the N-S movement of two continental crusts developed some structural elements related to the collision in the East Anatolian plate. The most important ones are the North Anatolian Fault Zone (NAFZ) and the East Anatolian Fault Zone (EAFZ) (Fig. 1(a)). Besides, the impacts of the collision are observed as inter-continental synthetic back thrust faults, right and left strike-slip faults located in a region extending from the BZSZ to approximately 200 km north of the BZSZ (Şengör *et al*., 1985). Additionally, the secondary tensional cracks and normal faults parallel, or at an angle, to the reverse faults developed during the thickening of the crust as a result of the collision of the continental plates. Similar features has been presented by Friedrich (1993) and Yin *et al*. (2008).

The Eastern Anatolia region, where all of these structural elements are observed, is defined as a compression region (Şengör and Kidd, 1979; Y lmaz *et al*., 1987; Y lmaz, 1990). The Lake Van Basin which is a ramp basin developed as a result of the activities of the thrust faults in the Eastern Anatolia compression region includes secondary normal faults and strike-slip faults (Şengör *et al*., 1985; Bozkurt, 2001; Koçyigit *et al*., 2001; Fig. 1(b)).

The earthquake area is known as a seismically-active region and is classified as a first category seismic zone in which damaging earthquakes occur (Lahn, 1949). The seismicity catalogue for the area was reported to be incomplete, particularly with regard to seismicity of a magnitude $M < 4$, because of the absence or scarcity of seismic recording stations in Eastern Turkey (Turkelli *et al*., 2003).

doi:10.5047/eps.2012.05.002

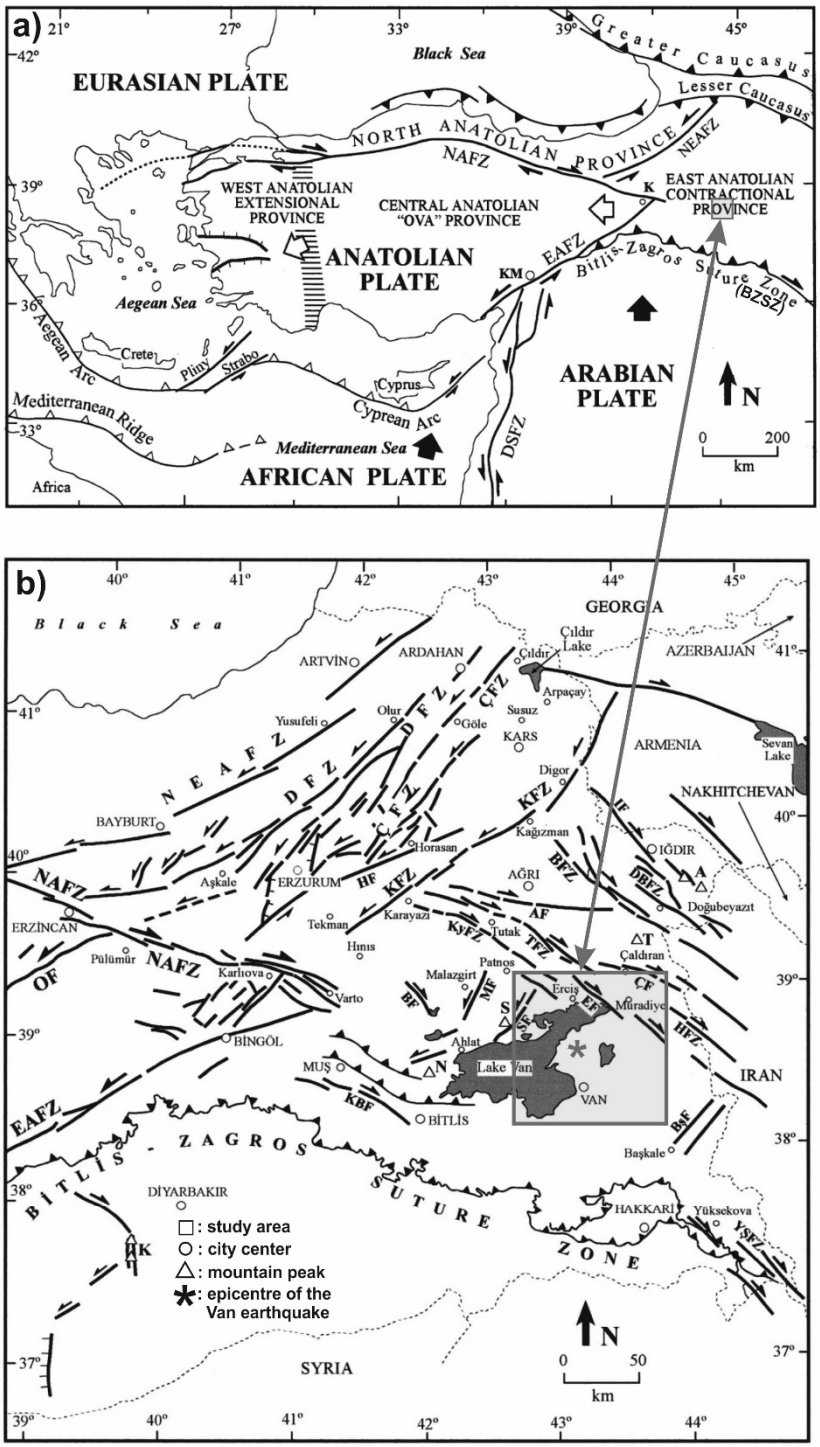

Fig. 1. (a) The general neotectonic map of Anatolia. K—Karl ova, KM—Kahramanmaraş, DSFZ—Dead Sea Fault Zone, EAFZ—East Anatolian Fault Zone, NAFZ—North Anatolian Fault Zone (Şengör *et al*., 1985; Barka, 1992; Bozkurt, 2001). (b) Neotectonic map of the East Anatolian and Van region. A—Agr Mountain, K—Karacadag, N—Nemrut Mountain, S—Süphan Mountain, T—Tendürek Mountain, AF—Agr Fault, BF—Bulan k Fault, ÇF—Çald ran Fault, EF—Erciş Fault, HF—Horasan Fault, IF—Igd r Fault, MF—Malazgirt Fault, OF—Ovac k Fault, SF—Süphan Fault, BFZ—Bal kl -lake Fault Zone, BsF—Başkale Fault, ÇFZ—Çobandede Fault Zone, DFZ—Dumlu Fault Zone, HFZ—Hasan Timur Fault Zone, KBF—Kavakbaş Fault, KFZ—Kag zman Fault Zone, DBFZ—Dogubeyaz t Fault Zone, KyFZ—Karayaz Fault, TFZ—Tutak Fault Zone, YSFZ—Yüksekova-Şemdinli Fault Zone, NEAFZ—Northeast Anatolian Fault Zone (Bozkurt, 2001).

Furthermore, historical and instrumental seismicity records prove that the area has produced a number of earthquakes from moderate to large magnitudes (Table 1).

The purpose of this study is to de ne the tectonic system that has deformed the region by using the surface rupture data, and fault plane solutions of the main shock and aftershocks of the 23 October, 2011, Van earthquake that occurred in the eastern Anatolian compression region. The source rupture processes of this earthquake were analyzed using teleseismic *P*-waves collected by the Data Management Center of the Incorporated Research Institutions for Seismology (IRIS-DMC). The source parameters of the 21

Table 1. Historical and Instrumental period earthquakes (Ergin *et al.*, 1967; Alsan *et al.*, 1975; Soysal *et al.*, 1981; Ambraseys, 1988; Eyidogan *et al.*, 1991; Turkelli *et al.*, 2003).

No	Date	Macroseismic Lat.–Lon. (°)	Instrumental Lat.–Lon. (°)	Remark	Intensity/Magnitude
1	02.04.1647	39.15–44.00		Van, Bitlis, Muş	IX
2	05.03.1871	38.50–43.40			5.5 (M_s)
3	30.05.1881	38.50–43.40		Van, Bitlis, Muş	7.3 (M_s)
4	10.02.1884	38.40–42.10			6.1 (M_s)
5	03.05.1891	39.15–42.50			5.5 (M_s)
6	28.04.1903	39.14–42.65		Malazgirt	7.0 (M_s)
7	27.01.1913		38.38–42.23		5.4 (M_s)
8	14.02.1915		38.80–42.50		5.6 (M_s)
9	20.11.1945		38.63–43.33	Van	5.5–5.8 (M_s)
10	03.09.1952		39.00–43.00		5.5 (M_s)
11	27.04.1966		38.13–42.52		5.6 (M)
12	24.11.1976		39.10–44.02	Çald ran	7.3 (M_s)
13	15.11.2000		38.40–42.92	Van	5.7 (m_b)

aftershocks ($3.5 < M < 5.7$) have been derived by using the rst motion polarities of regional P-waves collected by KOERI. The fault plane solutions of the earthquakes that occurred in the seismogenic zone of the continental crust were carried out in detail. The results of the fault plane solutions were compared with the surface rupture geometry to reveal the active tectonic model of the Lake Van Basin.

2. Field Observations

The Van earthquake resulted in a main surface rupture (MSR), along with secondary surface ruptures, in an area extending in a N-S direction from Erciş to Van and extending in an E-W direction from Bardakç Village to 4.5 km south east of Aş t Village, and around the western shore of Lake Erçek (Fig. 2). The MSR was accompanied with left-lateral tensional cracking, developed following the compression, with less than 300 m laterally (Dogan *et al.*, 2011).

The MSR of the Van earthquake was caused by a main fault that has a dominant thrust offset accompanied by minor left-lateral offsets in various locations (Fig. 3(a)). When the north dipping plane, obtained from the focal mechanism solutions of the main shock by various international earthquake centers, is considered as the main plane, a minor left lateral is noticeable. The eld observations of the MSR supported this focal mechanism solution. The overall strike of the MSR changes from N55°E to N70°E. This thrust fault is the primary fault plane with N60°E/65°NW strike and dip starting in Bardakç Village, located east of Lake Van on land. The strike of the MSR is N60°–65°E from Bardakç Village to the Van-Erciş Highway with no change in dip direction and dip angle (Fig. 3(b)). The MSR follows N65°–70°E in the east of the Van-Erciş Highway and is observed with minor left-lateral offset in 200-m zones from north to south in the Van organized industrial site. The total length of the MSR (between Bardakç and east of the Van-Erciş Highway) is about 8 km with a 0.15-m maximum thrust vertical offset and a 0.09-m left-lateral offset. The MSR is not observed beyond 4.5 km southeast of Aş t Village further east.

Another surface rupture of 4-km length, located between Kozluca and Yaln zagaç villages in the west of Lake Erçek, indicates a right step-over transpressional left-lateral strike-slip fault geometry (Fig. 3(c)). The strike of the second fault varies N-S and N15°E. It was mainly followed in elds and grasslands, so the left-lateral offset was only measured as 0.08 m at one location in the village of Yaln zagaç. This fault caused rockfalls at the northwest of Lake Erçek and does not continue northeast of the lake. In addition, triangular facets extending in a N-S direction and left-lateral offsets in the E-W ridges-valleys were observed between high rugged morphology and low plain morphology between the villages of Sat bey and Kolsatan.

Several secondary structural features of the region are observed in the northern block of the main fault. These features are seen in Erciş, and the villages of Gülsünler and Göllü, located around the Van-Erciş Highway. These secondary structural features were observed in Erciş with a N10°–40°E direction as en-echelon tensional ground cracks with a maximum 2-m zone (Fig. 3(d)). The maximum vertical offset was 0.3 m. Although the rupturing plane was not circular, down blocks were back-tilted to the rupturing plane. This surface rupture geometry is observed discontinuously in an east-west direction between the villages of Gülsünler and Göllü. The southern blocks, which moved downward, were observed along the secondary surface ruptures. The same type ruptures had been observed in a delta located in Gölcük-Kavakl near the western fault end of the 1999 Kocaeli (Turkey) earthquake, and was de ned as the Kavakl normal fault (Barka *et al.*, 2002). In addition to the secondary surface ruptures, landslides and liquefactions were widely observed in the northern block of the region (Fig. 3(e)).

3. Seismological Data Base

The number of digital broadband stations operated by The National Earthquake Monitoring Center of the Kandilli Observatory and Earthquake Research Institute (NEMC-KOERI) has been increasing since the devastating earthquake of 17 August, 1999, in Turkey. Therefore, it is possible to obtain reliable fault plane solutions for any area of Turkey, using either conventional methods such as rst motion polarities or using waveform inversion techniques.

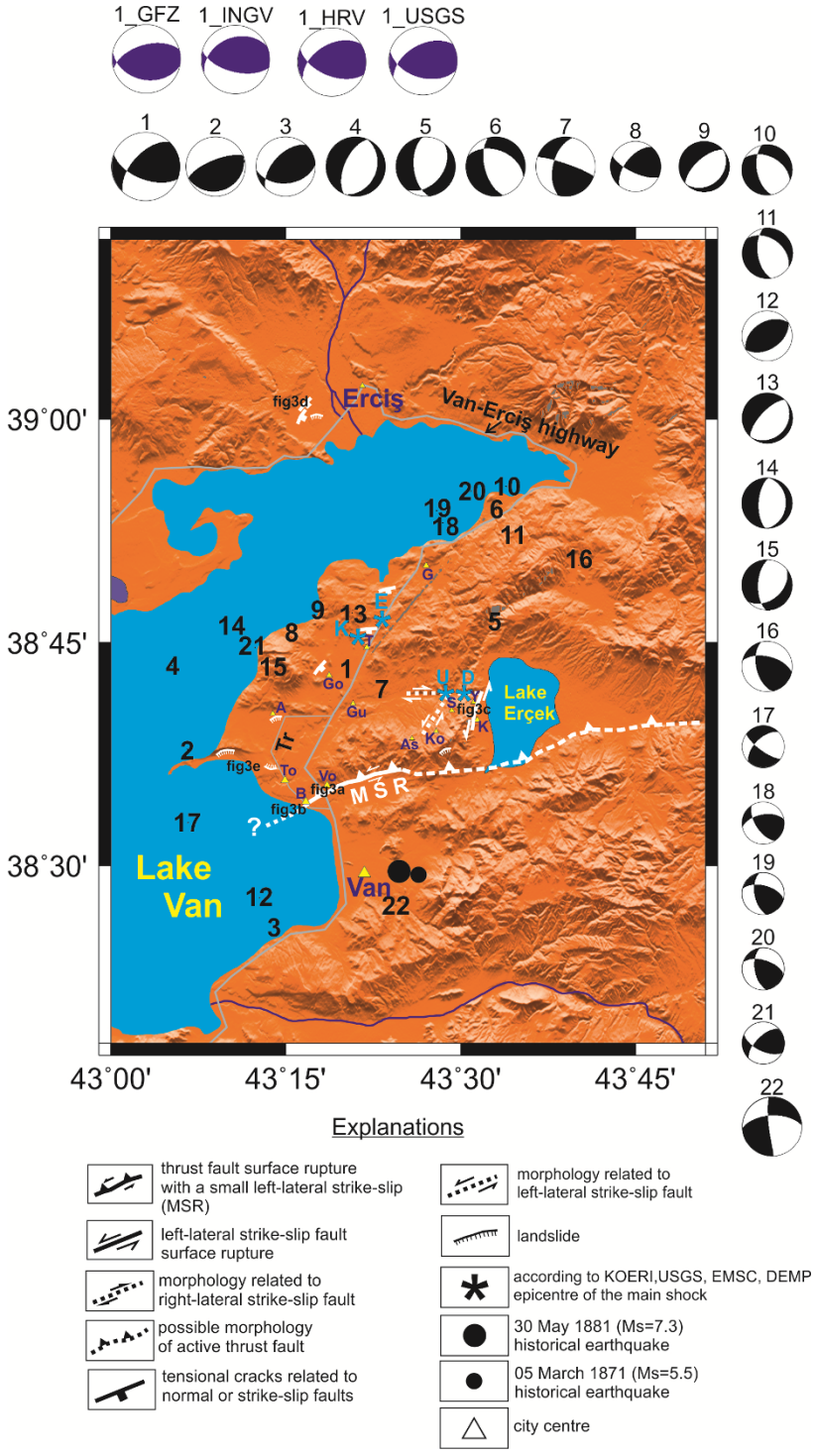

Fig. 2. The fault plane solutions of the main shock and 21 aftershocks of the Van earthquake with the surface ruptures which occurred during the earthquake, A: Alaköy, B: Bardakçı, Ko: Kolsatan, K: Kozluca, Y: Yalnızağaç, S: Satıbey, As: Aşıt, Gu: Gülsünler, Go: Göllü, To: Topaktaş, T: Tabanlı, Vo: Van organized industrial site. G: Gedikbulak, Tr: Topaktaş road, U: United States Geological Survey (USGS), D: Disaster and Emergency Management Presidency of Turkey (DEMP), E: European Mediterranean Seismological Centre (EMSC), K: Kandilli Observatory and Earthquake Research Institute (KOERI). Focal mechanisms reported by different agencies for the mainshock (event no. 1) are also shown on the top of the figure (GFZ: Deutsches GeoForschungsZentrum, Germany; INGV: Istituto Nazionale di Geofisica and Vulcanologia; HRV: Harvard University; USGS: United States Geological Survey. The ruptured parts are shown with the straight lines and unruptured parts are shown with the dashed lines, the numbers on the map and above the focal mechanism indicate events given in Table 3).

Broadband data with vertical components of teleseismic *P*-waves were retrieved from the Data Management Center of the Incorporated Research Institutions for Seismology (IRIS), selecting 35 stations with epicentral distances between 30° and 100° (Fig. 4). The data windowed at 50 seconds starting at 10 seconds before *P*-wave arrival and was integrated to displacement, and band-pass filtered between 0.002 Hz and 1.0 Hz. Figure 5 shows the depth of the seismogenic zone for the region, using the aftershocks ($M > 2.0$) which occurred within ten days of the main-

Fig. 3. (a) A view of left-lateral offset on a concrete block, caused by the MSR. (b) A view from the main surface rupture (MSR) on the Topaktaş road. The vertical thrust offset is approximately 0.1 m. (c) The NE-SW trending, left-lateral strike-slip fault surface rupture with transpressional component (push-up structures) on the west side of Lake Erçek. (d) The en-echelon shaped tensional cracks in Erciş. (e) View of the landslide and liquefactions near Topaktaş village.

shock. The data set was obtained from the KOERI catalog (http://www.koeri.boun.edu.tr/scripts/Sondepremler.asp).

4. Focal Parameters of the Main Shock and Aftershocks

The fault plane solutions were calculated by utilizing *P*-polarities running the *focmec* programs (Snoke *et al.*, 1984) for the mainshock and 21 aftershocks of the 23 October, 2011, Van earthquake. All available polarities from national seismic stations were carefully considered. The number of stations with unambiguous first arrival polarities varies from earthquake to earthquake, but events with fewer than 10 clear polarity readings were discarded, as were those with ambiguous polarities. The takeoff angles were calculated according to the same velocity structure used for the determined location (Table 2). The possible nodal planes which agree with the first motion polarities were searched, running the *focmec* program (Snoke *et al.*, 1984). The *P*-waves were converted to displacement in order to see the *P*-wave onsets better due to a low S/N ratio. Assuming the double-couple model for the seismic point source, *P*-polarities on displacement seismograms were then read. Polarity errors could be caused by low S/N ratio at stations near nodal planes, so called 'mislocations', or structural heterogeneity, biasing calculation of azimuth and take off angle and aliasing effects (Scherbaum, 1994). However, no polarity error was allowed in the solutions. Events with multiple acceptable solutions, indicating different mechanisms, or with faulting parameter uncertainties exceeding 20°, were not included in this study. The studied aftershocks have been re-located using digital broadband records. The epicenter coordinates of the after-

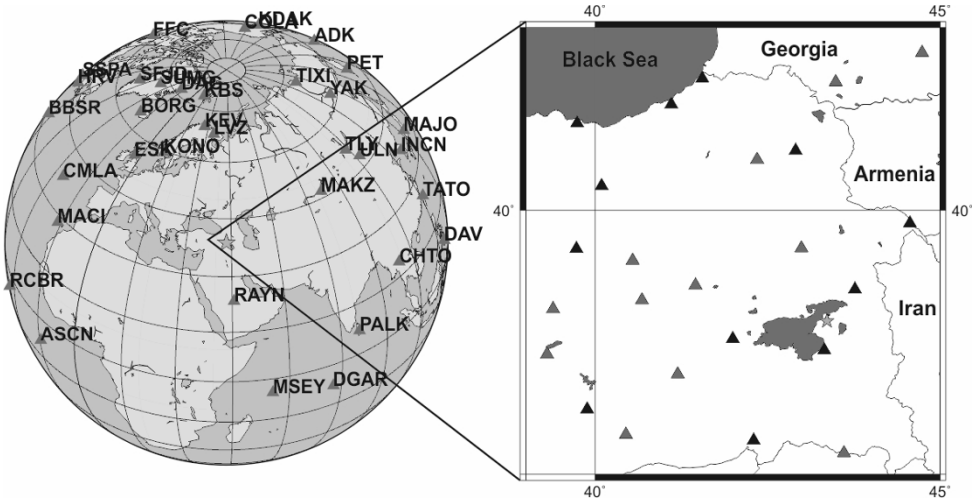

Fig. 4. Station locations used for the focal mechanism (right) and the slip distribution analysis (left). The yellow star indicates the epicenter, and the triangles are the stations used for the relocation of the analyzed aftershocks (red triangles are used for the rst motion solution of the mainshock).

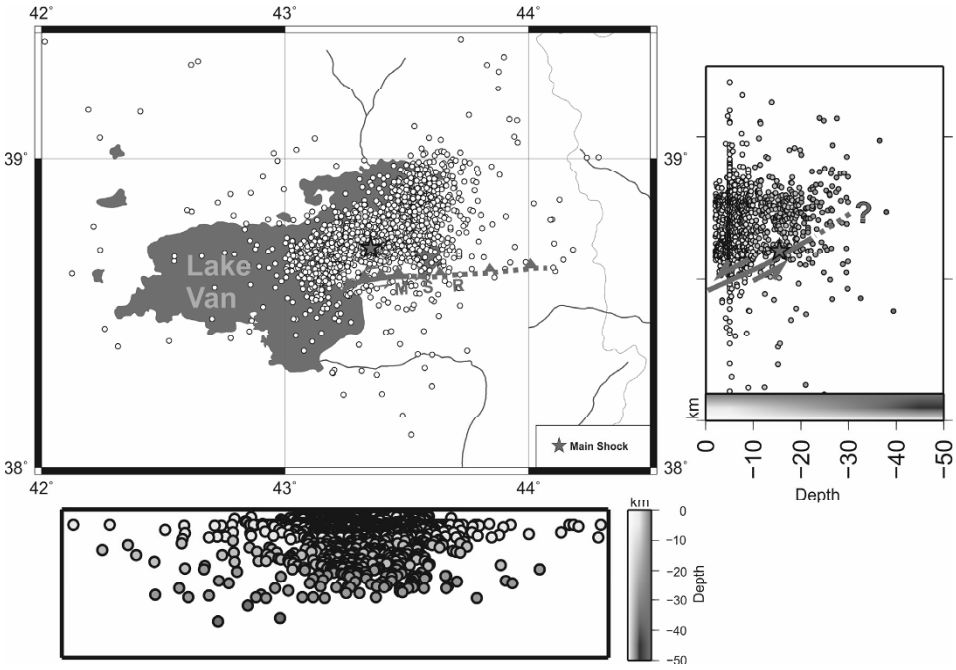

Fig. 5. Distributions of the 23 October, 2011, Van earthquake (main shock shown by the red star) aftershocks and their depths.

shocks given by KOERI were preliminary, so the P- and S-wave phases were re-read to reduce the horizontal (ERH) and depth (ERZ) error. We calculated hypocenter locations by using P-wave arrival times of at least ten stations and also the S-wave arrival times of at least two stations. The aftershocks were processed using HYPO71 (Lee and Valdes, 1985) for the hypocenter determination. However, 1–2-km differences were obtained between the rst solutions and ERH and ERZ. The digital data and error values are available http://barbar.koeri.boun.edu.tr/sismo/zKDRS/zzTReventIndex.asp for the preliminary results.

The rst motion polarity solution of the mainshock represents the initial movement at the focus, whereas the moment tensor solution represents the source parameters of the large slip area. This explains the difference between our rst motion solution and moment tensor solutions reported by different agencies. When the fault plane solutions with tensor analysis issued by other institutions are plotted on the sphere, including the stations utilized for the rst motion polarity analysis, it is clear that they could not precisely distinguish the compression and dilatation (Fig. 6). Therefore, the fault plane solutions that were obtained by

Table 2. 1-D velocity models derived by Kalafat *et al*. (1987) and used in this study.

Depth (km)	V_p (km/s)	V_s (km/s)
0.00	4.50	2.60
5.40	5.91	3.10
31.6	7.80	4.50
89.2	8.30	4.80

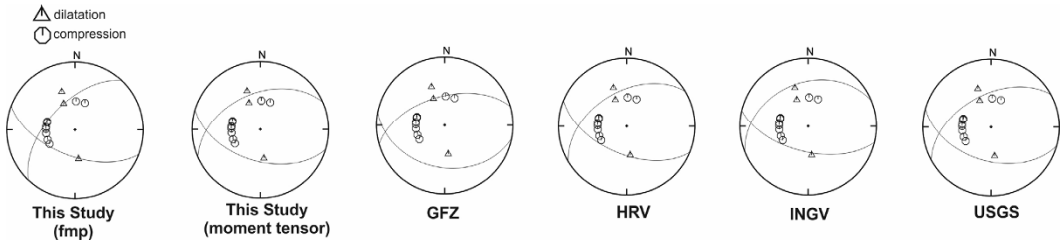

Fig. 6. Focal mechanism of the main shock obtained by P-wave first motion and moment tensor analysis, and results published by other institutes (see Fig. 2 for abbreviations).

the first motion polarity analysis represent the rupture initiation better than the moment tensor analysis. However, the fault model based on the moment tensor solution is more appropriate than the fault model estimated from the focal mechanism by the initial P-wave polarity, since the focal mechanism by the P-wave polarities represents only the initial rupture process during the mainshock. Thus, the focal mechanisms obtained by the moment tensor solution in the inversion method were used. Indeed, several source inversion studies, using teleseismic data, assumed fault models based on moment tensor solutions (e.g. Kikuchi *et al.*, 2000; Yagi, 2004; Yagi *et al.*, 2004).

In addition, the fault plane solutions were compared with the surface ruptures mapped in the field. The strike-slip faults along with the thrust faults that were also determined by the fault plane solutions of the aftershocks, and tensional cracks possibly related to the normal or left-lateral strike-slip faults, were observed especially in the overlapping northern block due to the NW-SE compression among the micro-scaled continental plates. A similar fault plane solution pattern was observed in the 1952 Kern county earthquake which occurred on the Pleito thrust fault in the north of the San-Andreas fault, which presented both normal and thrust faults with a strike-slip offset component (Webb and Kanamori, 1985).

5. Teleseismic Waveform Analysis of the Main Shock

To determine the focal mechanisms for the 23 October, 2011, Van earthquake from teleseismic broadband data, we introduced a time-domain iterative inversion method developed by Kikuchi and Kanamori (1991). We chose 35 stations and picked up vertical P-waves for the analysis. The azimuthal coverage is good enough to resolve the focal mechanism and also some details of the moment-release distribution. With the approximation of a single point source, we determined the fault mechanism so that predicted waveforms best fit the observed ones (Fig. 7(c)). We used teleseismic broadband P-wave data recorded at IRIS-DMC stations retrieved via internet. The data were band-passed between 0.01–0.5 Hz using a zero phase-shift Butterworth band-pass filter to remove long-period drift and high-frequency noise, then the data was converted to a ground displacement with a sampling interval of 0.2 s.

The Green's functions have been computed using the Kikuchi and Kanamori (1991) method. The ray is incident almost perpendicularly on the receiver at teleseismic distances, and is not affected by near source crustal effects, so we used a standard JB crustal model to compute the theoretical waveforms. A Q filter was used with the attenuation time constant $t_p = 1$ s for P-waves and $t_s = 4$ s for S-waves. The moment tensor solution indicate that the 23 October, 2011, Van earthquake has a reverse faulting mechanism with a small amount of left-lateral strike-slip component (Fig. 7(b)).

To obtain the slip distribution, a single fault plane was assumed for the waveform analysis. The initial size of the fault plane was taken to be 75 km × 25 km from the aftershock distribution, and the rupture was assumed to start at the hypocenter of the mainshock. According to the right-hand rule, the strike and dip angle-directions were assumed to be 246° and 46°NW respectively, referring to the moment tensor solution obtained in this study.

Theoretical Green's functions were computed for simple layers and were referred to the Jeffreys-Bullen model, using Kikuchi and Kanamori's (1991) method for all stations; this is due to the fact that it is generally expected that the observed seismograms are less affected by local site effects in the teleseismic range. The spatiotemporal distribution of slip on the fault plane was inverted by the teleseismic body-wave inversion program developed by Yoshida *et al.* (1996) and Yagi and Kikuchi (2000). For discretization in space, the fault plane was divided into 15 in the strike direction and into 5 in the down-dip direction (making a total of 75 subfaults with an area of 5 km × 5 km). The slip rate function of each subfault is expanded into a series of 2 triangle functions with a rise time of 1.0 seconds. The rupture front velocity of 3.0 km/s was selected by trial and error, which determines the initiation time of the basis function at each subfault, that minimizes the residuals between the observed and predicted waveforms. To suppress instability or excessive complexity, a smoothing constraint was applied to differences in the moment release.

The results for the slip distribution obtained by teleseismic waveform inversion are shown in Fig. 8. Figure 9 shows the observed and predicted waveforms. The overall matching between the predicted and observed waveforms is very good. The total seismic moment is calculated as 5.53×10^{19} N m ($M_w = 7.1$), similar to the seismic moment of 5.8×10^{19} N m derived by the Deutsches GeoForschungsZentrum, Germany-GFZ, 6.40×10^{19} N m calculated by KOERI, 7.1×10^{19} N m calculated by HRV, and 5.6×10^{19} N m calculated by USGS (http://www.emsc-csem.org/Earthquake/tensors.php?id=239856&id2=cz772;INFO). The main rupture is located around the initial break point and the max-

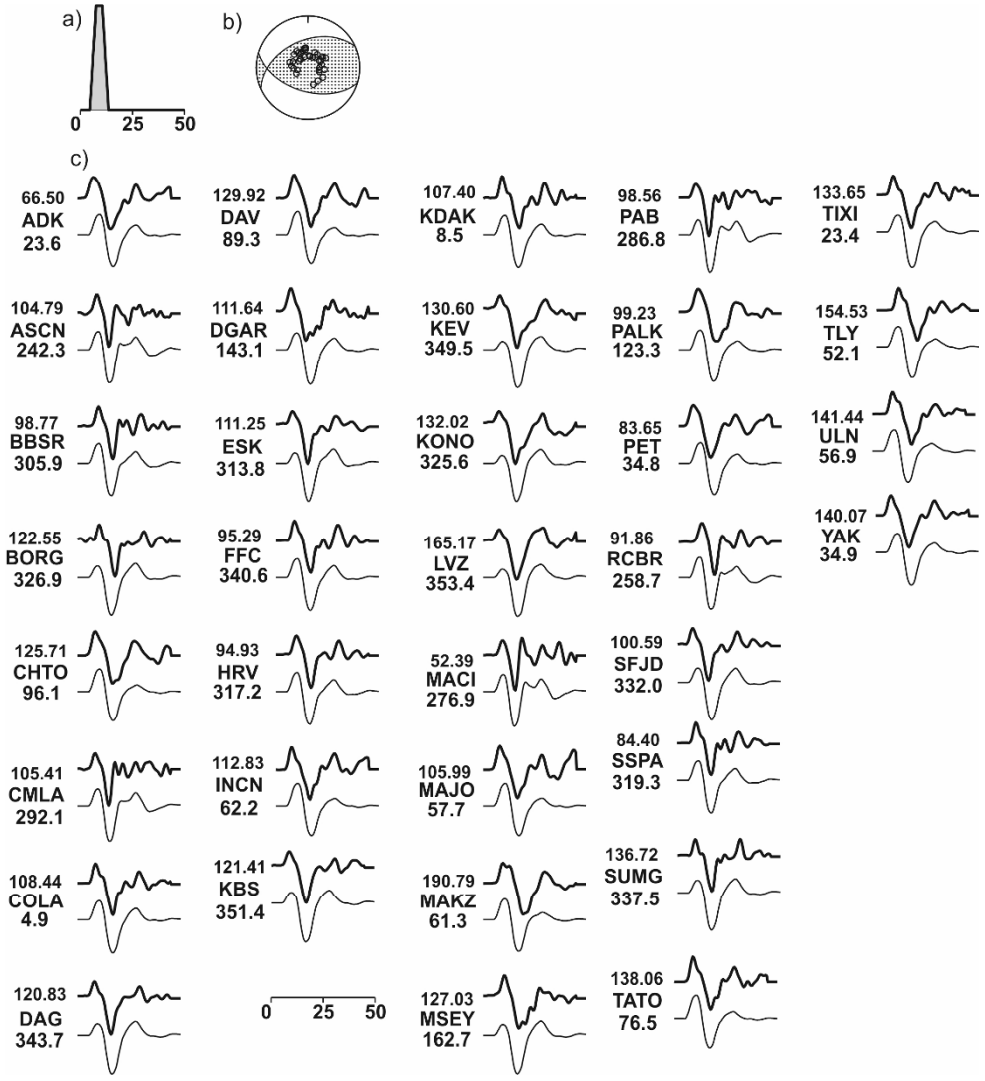

Fig. 7. Focal mechanism obtained using the Kikuchi and Kanamori (1991) method, (a) source time function, (b) obtained focal mechanism, (c) waveform tting. The upper seismograms are observed and the lower seismograms are calculated. The number above the station code is the peak-to-peak amplitude of the observed waveforms (micro-meter) and the numbers below indicate the azimuths of the stations.

imum slip is 3.6 m, if the shear modulus is assumed to be 30 GPa. The size of the main fault was about 40 km in length and 20 km in width, and the duration of rupture was about 19 seconds with $M_w = 7.1$. The average stress drop $\Delta\sigma = 6.1$ MPa is comparable to a typical stress drop value of 3 MPa for inter-plate earthquakes (Kanamori and Anderson, 1975).

In the total slip distribution, a large asperity area can be seen with a large slip in the hypocentral area of the fault plane. The rupture is very smooth and gradually expands near the hypocenter and propagates bilaterally in the directions northeast and southwest (but mainly to the southwest). The main moment release areas are located at and around the hypocenter. The rupture front also reached a shallower part of the fault plane (asperity area) about 9 seconds after the rupture initiation. In the moment-rate function, a small peak occurs after about 15 s. This peak is due to asperity in the lower corner of the fault plane (Fig. 8(d)). In some broadband seismograms presented in Fig. 9, this peak is recognizable, too. According to these results, an asperity was broken at 15 s after the focal time of the main shock at a distance of about 40 km away from the hypocenter. A barrier with higher stress (or lower stress) and with a width of about 15 km was located between the asperity and the main slip area. The rupture jumped over this barrier with a velocity comparable to the rupture velocity.

The distribution of the slip vectors indicates that a thrust fault mechanism with a small left-lateral strike-slip component (assuming the NE-SW plane is the active plane) occurred near the hypocenter and in deep parts. However, a small left lateral strike-slip is dominant in shallow parts of the fault plane mainly NE of the epicenter. The moment release and displacements rates in the shallower parts of the fault plane are smaller than the deeper parts of the fault plane. This situation could reduce the chances of a continuous surface rupture. If the rupturing of the fault plane reached the surface, the left-lateral strike-slip component could be mainly seen at the northeast of the main fault.

6. Tectonic Model and Interpretations

The ophiolitic rocks emplaced to the Lake Van Basin along the thrust planes during the Paleotectonic period (be-

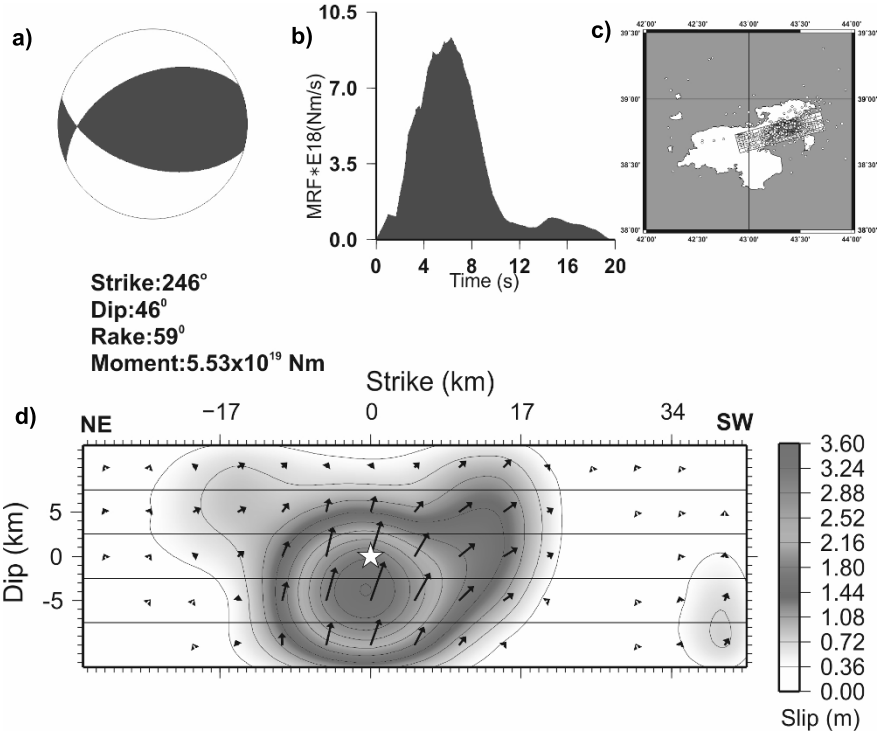

Fig. 8. Slip model from inversion of teleseismic waves: (a) focal mechanism, (b) moment rate function, (c) map view of the slip distribution (white circles indicate the aftershocks recorded within the first 24 hours), (d) slip distribution on the fault. The white star indicates the focus.

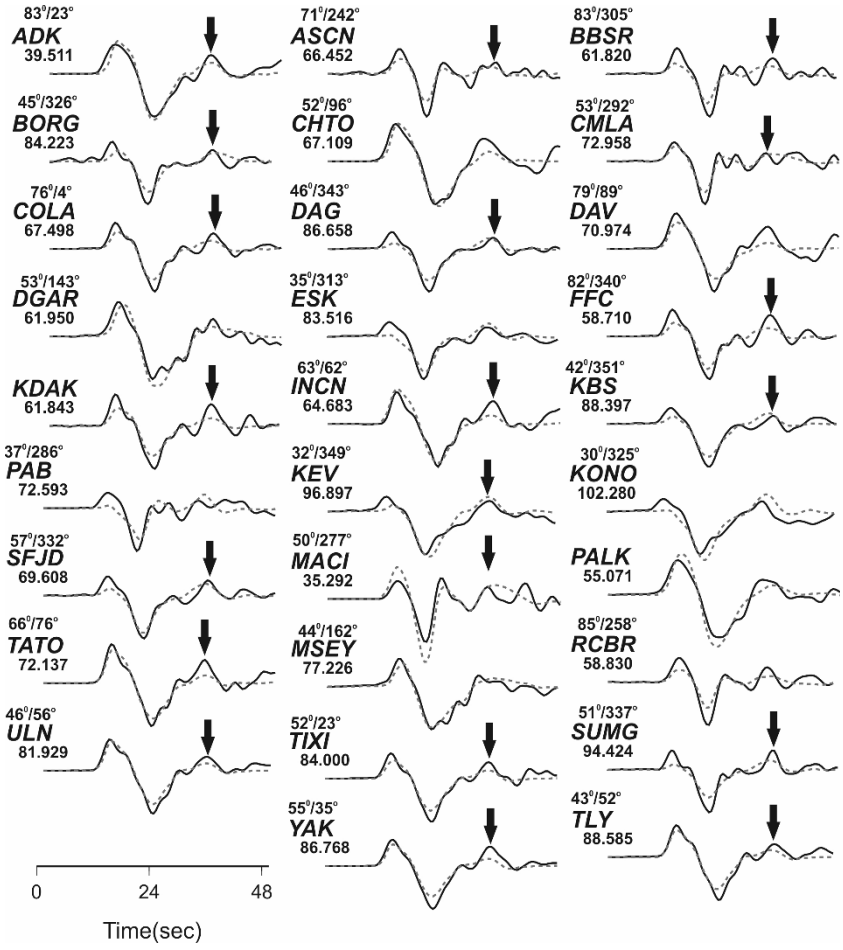

Fig. 9. *P*-wave waveform fits for the inversion, with observed and calculated waveforms shown as black and red lines, respectively. The number below the station code is the peak-to-peak amplitude of the observed waveforms (micro-meter). The numbers above indicate the distance and azimuth of the station, respectively. The arrows correspond to a small peak that occurred in the moment-rate function after about 15 s.

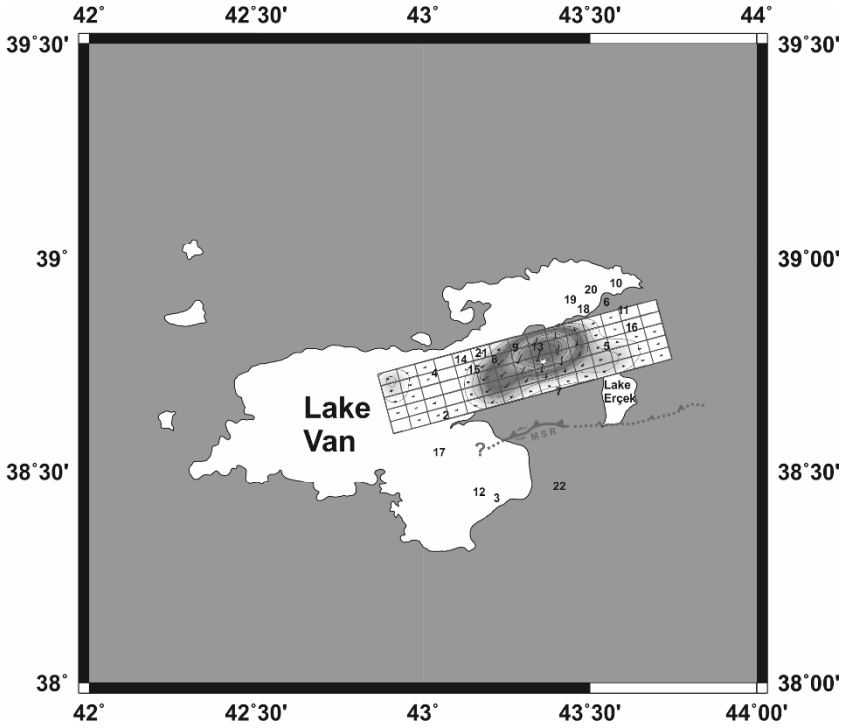

Fig. 10. Main shock slip distribution and analyzed aftershocks with the MSR (the numbers indicate the events given in Table 3, see Fig. 2 for symbols and abbreviations).

fore Neogene) constituted the rugged mountainous morphology in the region (Y lmaz *et al.*, 1993; Parlak *et al.*, 2000). This continental-continental collision type plate motion creates thrust faults with lengths less than the length of the BZSZ. Continuation of the compression during the Neotectonic period in the region developed several folds and thrust faults in the Neogene and Quaternary units deposited in the Lake Van Basin.

The thrust faults in the Lake Van Basin have the potential to produce earthquakes with magnitude greater than six. The thrust faults cut the Plio-Quaternary deposits especially in the north of Van city center (Örçen *et al.*, 2004). Thereby, these faults are likely to be active. Additionally, the minimum length of these faults is about 10 km, so each of these faults has the potential to generate an earthquake of magnitude greater than six ($M > 6$) (Wells and Coppersmith, 1994). One of the thrust faults, which has a fault plane dipping towards the NW, ruptured in the Van Lake Basin and created the Van earthquake. This rupture, which took place along the intra-continental thrust fault, developed secondary structural features such as left-lateral strike-slip faults with transpressional component and tensional cracks. The reason for this is that the widening areas related to the NE-SW left-lateral faulting could occur as a result of the NW-SE compression of the region. The fault-plane solutions of the main shock and the eld observations proved that the 23 October, 2011, Van earthquake was generated by an intra-plate thrust fault with a NE strike and NW dip. Additionally, the rupture of this fault plane developed the secondary faults and created the aftershocks and several tensional cracks on the ground surface or beneath the ground surface.

7. Conclusion and Discussions

This study has investigated the rupture process of the 23 October, 2011, Van (Turkey) earthquake by the inversion of teleseismic waveform analysis and its tectonic implications. The teleseismic data set does not provide details of the slip distribution, but it provides the same general characteristics as other data sets such as near eld, or strong ground-motion, data (Hartzell and Heaton, 1983; Yagi *et al.*, 2004). Therefore, we discuss the general features of the rupture process and compare the focal mechanisms of the analyzed earthquakes with eld observations.

The initiation of rupture is usually described by the rst motion polarity solution. However, the rupture direction could change during large earthquakes. The entire rupturing is modeled by slip-distribution modeling, which models the waveform. Therefore, the moment tensor solution is more suitable than the rst motion polarity solution in terms of representing the entire rupturing process. Additionally, the strikes of the fault planes obtained from the moment tensor solutions are more consistent with the main surface rupture. The difference between the directions of the fault planes obtained from the rst motion polarity solution and the moment tensor solution indicates that the direction of the rupture initiation is different from the entire rupture propagation.

The inverted source process model shows that a large asperity was located on the hypocentral area on the fault plane; with a maximum slip about 3.6 m. The rupture was very smooth and gradually expanded near the hypocenter and propagated bilaterally in the direction of northeast and southwest, but mainly to the southwest. The rupture process of the 23 October, 2011, Van earthquake is characterized by a smooth and bilateral rupture.

Table 3. First motion results of the focal mechanism of the studied earthquakes.

No	Date (dd/mm/yy)	Origin time (hr:mm:s)	Location (°) Lat.–Lon.	ERH (km)	ERZ (km)	Depth (km)	Mag	Strike	Dip	Rake
1	23/10/11	10:41:21	38.7188–43.3367	3.3	1.8	15.0	7.1*	246	46	59
2	23/10/11	20:45:34	38.6345–43.0775	2.7	0.5	5.0	5.7+	248	71	90
3	09/11/11	19:23:34	38.4295–43.2342	2.6	0.5	5.8	5.6+	223	55	63
4	08/11/11	22:05:50	38.7241–43.0870	0.9	0.5	4.3	5.5+	203	59	−88
5	25/10/11	14:55:08	38.7733–43.5468	3.2	1.0	5.0	5.4+	38	41	−54
6	29/10/11	22:42:22	38.8985–43.5503	0.9	0.2	5.0	5.3+	165	60	−56
7	23/10/11	18:10:45	38.6980–43.3873	3.5	0.5	5.0	5.0+	289	82	35
8	23/10/11	18:53:48	38.4072–43.3383	3.3	1.4	5.0	4.9+	219	57	25
9	23/10/11	19:06:06	38.7868–43.2960	3.7	0.8	5.0	4.9+	228	64	−90
10	06/11/11	02:43:12	38.9243–43.5650	1.2	0.3	5.0	4.9+	169	57	−54
11	02/11/11	04:43:20	38.8735–43.5695	1.3	0.3	5.0	4.8+	171	58	−61
12	09/11/11	22:38:18	38.4508–43.2085	1.9	0.7	5.0	4.5+	238	43	90
13	23/10/11	19:43:25	38.7835–43.3447	4.1	0.9	5.0	4.4+	223	68	−90
14	24/10/11	22:13:31	38.7710–43.1790	1.2	0.4	2.1	4.4+	183	63	−90
15	24/10/11	18:52:16	38.7263–43.2247	1.9	0.4	2.5	4.2+	50	41	−49
16	25/10/11	03:28:51	38.8368–43.6687	8.9	1.9	2.2	3.7+	283	57	43
17	25/10/11	00:16:40	38.5482–43.1103	3.7	1.4	5.0	3.7+	126	74	−34
18	24/10/11	20:15:49	38.8840–43.4742	0.9	0.3	5.0	3.6+	259	56	36
19	25/10/11	00:26:26	38.8977–43.4658	4.0	0.9	5.0	3.6+	285	57	42
20	24/10/11	16:24:19	38.9192–43.5143	0.4	0.1	3.7	3.6+	289	56	43
21	25/10/11	02:39:38	38.7445–43.2055	1.3	0.5	4.0	3.5+	115	61	146
22	30/11/11	00:47:21	38.5090–43.4058	2.6	1.2	2.8	5.0+	174	81	−32

ERH: Horizontal error, ERZ: Vertical error, *Moment magnitude (M_w) obtained by waveform inversion, +Local magnitude (M_L).

The aftershocks in the region are accumulated between the villages of Gedikbulak and Alaköy and have a NE-SW spread (see Fig. 2). The majority of the aftershocks occurred on the overlapping northern block and on or around the main thrust fault plane (Fig. 10). The main faulting plane of the entire faulting process could be located under the surface, while the surface ruptures continue east of the study area. The majority of the aftershocks investigated in this study have a strike-slip component, but the dominant component of the MSR is thrust. The normal and thrust aftershocks are related to the rupturing of the secondary faults created by the NW-SE compression, especially in the northern block. The Van earthquake was a result of the rupturing of a main thrust fault plane in the NE direction and with a 58°NW dip. This rupturing caused secondary intra-plate tensional cracks, left-lateral strike-slip faults on the northern block and a secondary right-lateral strike-slip fault with E-W direction obtained from the fault plane solution of the aftershock numbered 22 in Table 3, on the southern block. Both right-lateral and left-lateral strike-slip faults can develop in pure compressional areas (Philip *et al*., 1989). However, some of those faults could be unobservable on the surface. The fault plane solution of the aftershock numbered 22 is an example of this.

The surface ruptures observed from Erciş to Alaköy located on the northern block of the main thrust fault were defined as tensional cracks. These surface ruptures could be the structural products of a transtensional left-lateral strike-slip fault, and is an indication of intra crust deformation and suits with the direction of the aftershock pattern. The origin of the tensional cracks observed in the region could be explained by either normal faults or transtensional components, especially of left-lateral strike-slip faults. Both fault types are secondary and "intra-plate" with limited lateral continuation. In other words, the activities of these faults are directly related to the rupturing of the thrust faults in the region. In some regions of the world, there are several examples of both normal and strike-slip faults which developed due to a N-S compression of the region. For example, normal faults that were parallel and semi-parallel to the strike of the Vergent thrust fault System (WTS) developed during the 4 July, 2001, earthquake in the Altiplano region of north Chili in the overlapping continental plate (Somoza, 1998; Farias *et al*., 2005). In addition, it was indicated that the normal faults could be transtensional faults that created the pull-apart basins in the same region (David *et al*., 2002). Another example is that several normal faults parallel and semi-parallel to the thrust faults in the north and northeast of the Alborian Basin in Spain developed contemporarily with the overthrust (Roca *et al*., 2006). Additionally, a graben was formed by the normal faults parallel to the reverse faults of the continental thrust zone and strike-slip faults developed concurrently due to regional compression in the West Europe Carpathian region. Although the reverse faults were dominant in the southeast of the East Carpathian region, normal faults with the same strike were observed in the northeast region (Oszczypko *et al*., 2006; Picha, 2011). The small-scale normal faults parallel to the reverse fault planes that occurred along with the raising of the hanging wall, and shortening, were determined by the tectonic model of the 2008 Wenchuan earthquake in the Tibet Plateau (China) (You-Li *et al*., 2010). These normal faults developed as a consequence of both heterogenic stress distribution in the seismogenic zone and thickening

and shortening of the overlapping block.

The surface appearances of the normal faults based on the fault plane solutions of the aftershocks are in the form of tensional ground cracks in the study area. These tensional cracks are the secondary structural features developed on the overlapping northern block. The development of the tensional cracks are either related to the normal faults created by the thickening and contraction of the northern block, or the rupturing of the transtensional parts of the intra-continental strike-slip faults created by the compression.

Acknowledgments. We would like to thank the Rector of Kocaeli University, Prof. Dr. Sezer Ş. Komsuoglu, and the retired dean of the Engineering Faculty, Prof. Dr. Savaş Ayberk, and Prof. Dr. Mithat F rat Özer, for their support, and the Rector of Van 100. Y l University, Prof. Dr. Peyami Battal, for providing us transportation and accommodation during our stay in Van. Also, a special thanks is extended to Assistant Prof. Dr. Özkan Coruk for his contribution during the of ce work and Serdal Karaagaç for his contributions during the eld and of ce works, and John Pyle for his reviewing effort. We also thank two anonymous reviewers for their helpful comments that improved the manuscript.

References

Alsan, E., L. Tezucan, and M. Bath, An earthquake catalog for Turkey for the interval 1913–1970, Kandilli Obs., Istanbul and Seismological Inst. Rept. 7-75, 1975.

Ambraseys, N. N., Engineering seismology, *Int. J. Earthq. Eng. Struct. Dyn.*, **17**, 1–105, 1988.

Barka, A. A., The North Anatolian Fault Zone, *Ann. Tectonicae*, **6**, 174–195, 1992.

Barka, A., H. S. Akyüz, E. Altunel, G. Sunal, Z. Çakir, A. Dikbas, B. Yerli, R. Armijo, B. Meyer, J. B. de Chabalier, T. Rockwell, J. R. Dolan, R. Hartleb, T. Dawson, S. Christofferson, A. Tucker, T. Fumal, R. Langridge, H. Stenner, W. Lettis, J. Bachhuber, and W. Page, The surface rupture and slip distribution of the 17 August 1999 Izmit earthquake (M 7.4), North Anatolian fault, doi:10.1785/0120000841, *Bull. Seismol. Soc. Am.*, **92**(1), 43–60, 2002.

Bozkurt, E., Neotectonics of Turkey—a synthesis, *Geodinamica Acta (Paris)*, **14**, 3–30, 2001.

David, C., J. Martinod, D. Comte, G. Herail, and H. Haessler, Intracontinental seismicity and Neogene deformation of the Andean forearc in the region of Arica (18.5°S–19.5°S), paper presented at 5th International Symposium on Andean Geodynamics, Inst. de Rech. pour le Dev. (IRD), Toulouse, France, 2002.

DEMP (Disaster and Emergency Management Presidency of Turkey), http://www.deprem.gov.tr/sarbis/Shared/WebBelge.aspx?param=105, 2011.

Dewey, J. F., M. R. Hempton, W. S. F. Kidd, F. Şaroglu, and A. M. C. Şengör, Shortening of continental lithosphere: the neotectonics of Eastern Anatolia—a young collision zone, in *Collision Tectonics, Geol. Soc. London Spec. Pub. 19* (R.M. Shackleton volume), edited by M. P. Coward and A. C. Ries, 3–36, 1986.

Dogan, B., A. Karakaş, and S. Karaagaç, 23.10.2011 tarihli (Bardakç - Kozluca köyleri) Ön Degerlendirme Raporu, University of Kocaeli, Engineering Faculty, Department of Geological Engineering, Izmit-Kocaeli, 2011 (in Turkish).

Ergin, K., U. Guolu, and Z. Uz, A catalog of earthquakes for Turkey and surrounding areas, *Tech. Univ. Istanbul Mining Eng. Fac., Publ. No. 24*, 74 pp., 1967.

Eyidogan, H., U. Güçlü, Z. Utku, and E. Degirmenci, Türkiye Büyük Depremleri Makro-Sismik Rehberi (1990–1988), *İTÜ Maden Fak. Jeofizik Müh. Böl., Istanbul*, 1991 (in Turkish).

Farias, M., R. Charrier, D. Comte, J. Martinod, and G. Herail, Late Cenozoic deformation and uplift of the western ank of the Altiplano: Evidence from the depositional, tectonic, and geomorphologic evolution and shallow seismic activity (northern Chile at 19^0 30^1S), *Tectonics*, **24**, TC4001, doi:10.1029/2004TC001667, 2005.

Friedrich, A. M., Analysis of the Mesozoic Wahwah thrust system with Cenozoic extensional overprint, southwestern Utah, 112 p., M.S. thesis, University of Utah, Salt Lake City, 1993.

Hartzell, S. H. and T. H. Heaton, Inversion of strong ground motion and teleseismic waveform data for the fault rupture history of the 1979 Imperial Valley, California, earthquake, *Bull. Seismol. Soc. Am.*, **73**, 1553–1583, 1983.

http://www.koeri.boun.edu.tr/scripts/Sondepremler.asp (visited date: 01.12.2011).

Kalafat, D., C. Gürbüz, and B. Üçer, Bat Türkiye'de Kabuk Yap s ve üst manto araşt r lmas , *Deprem Araştırma Bülteni*, **59**, 43–64, 1987 (in Turkish).

Kanamori, H. and D. L. Anderson, Theoretical basis of some empirical relations in seismology, *Seism. Soc. Am.*, **65**(5), 1073–1095, 1975.

Kikuchi, M. and H. Kanamori, Inversion of complex body waves—III, *Bull. Seismol. Soc. Am.*, **81**, 2335–2350, 1991.

Kikuchi, M., Y. Yagi, and Y. Yamanaka, Source process of Chi-Chi, Taiwan earthquake of September 21, 1999 inferred from teleseismic body waves, *Bull. Earthq. Res. Inst. Univ. Tokyo*, **75**, 1–13, 2000.

Koçyigit, A., A. Y lmaz, A. Adamia, and S. Kuloshvili, Neotectonics of East Anatolian Plateau (Turkey) and Lesser Caucasus: Implication for transition from thrusting to strike-slip faulting, *Geodinamica Acta*, **14**, 177–195, 2001.

KOERI, http://www.koeri.boun.edu.tr/sismo/indexeng.htm, 2011 (visited date: 01.12.2011).

Lahn, E., Seismological investigations in Turkey, *Bull. Seismol. Soc. Am.*, **39**, 67–71, 1949.

Lee, W. H. K. and C. M. Valdes, *HYPO71PC: A Personal Computer Version of the HYP071Earthquake Location Program*, USGS, Open File Report, 1–28, 1985.

Örçen, S., A. U. Tolluoglu, O. Köse, T. Yakupoglu, Y. Çiftçi, M. A. Iş k, L. Selçuk, S. Üner, C. Ozkaymak, I. Akkaya, A. Ozvan, A. Saglam, M. Baykal, Y. Özdemir, T. Üner, O. Karaoglu, C. Yeşilova, and V. Oyan, Van Şehri kentleşme alan nda yüzeyleyen Pliyo-Kuvaterner çökellerinde sedimantolojik özelliklerin ve aktif tektonizman n depremsellige yönelik incelenmesi, TUBITAK, Proje no: YDABAG-101Y100 (VAP-10), pp. 59–84, 2004 (in Turkish).

Oszczypko, N., P. Krzywiec, I. Popadyuk, and T. Peryt, Carpathian foredeep basin (Poland and Ukraine): Its sedimentary, structural, and geodynamic evolution, in *The Carpathians Picha 979 and Their Foreland: Geology and Hydrocarbon Resources: AAPG Memoir 84*, edited by J. Golonka and F. J. Picha, pp. 293–350, 2006.

Parlak, O., M. Delaloye, H. Kozlu, V. Höck, and Ö. F. Çelik, Geochemistry and tectonic setting of the Yüksekova ophiolite from the South-East Anatolian Orogenic Belt, *International Earth Sciences Colloquium on the Aegean Region (IESCA-2000)*, 25–29 Eylül, 240, 2000.

Philip, H., A. Cisternas, A. Gvishiani, and A. Gorshkov, The Caucasus: An actual example of the initial stages of continental collision, *Tectonophysics*, **161**, 1–21, 1989.

Picha, F. J., Late orogenic faulting of the foreland plate: An important component of petroleum systems in orogenic belts and their forelands, *AAPG Bull.*, **95**(6), 957–981, 2011.

Reilinger, R., S. McClusky, P. Vernant, S. Lawrence, S. Ergintav, R. Cakmak, H. Ozener, F. Kadirov, I. Guliev, R. Stepanyan, M. Nadariya, G. Hahubia, S. Mahmoud, K. Sakr, A. Abdullah, D. Paradissis, A. Al-Aydrus, M. Prilepin, T. Guseva, E. Evren, A. Dmitrotsa, S. V. Filikov, F. Gomez, R. Al-Ghazzi, and G. Karam, GPS constraints on continental deformation in the Africa-Arabia-Eurasia continental collision zone and implications for the dynamics of plate interactions, *J. Geophys. Res.*, **111**, B05411, doi:10.1029/2005JB004051, 2006.

Roca, E., S. Maura, and A. K. Hemin, Polyphase deformation of diapiric areas in models and in the eastern Prebetics (Spain), *AAPG Bulletin*, **90**(1), 115–136, 2006.

Şaroglu, F. and Y. Y lmaz, Dogu Anadolu'da Neotektonik Dönemdeki Jeolojik Evrim ve Havza Modelleri, *MTA Genel Müdürlüğü, Jeoloji Etütleri Dairesi*, Ankara, 1986 (in Turkish).

Scherbaum, F., Modelling the Roermond earthquake of 1992 April 13 by stochastic simulation of its high-frequency strong ground motion, *Geophys. J. Int.*, **119**, 31–43, 1994.

Snoke, J. A., J. W. Munsay, A. G. Teague, and G. A. Bollinger, A program for focal mechanism determination by combined use of polarity and SV-P amplitude ratio data, *Earthq. Notes*, **55/3**, 15, 1984.

Somoza, R., Updated Nazca (Farallones)-South America relative motions during the last 40 My: Implications for mountain building in the central Andes region, *J. S. Am. Earth Sc.*, **11**, 211–215, 1998.

Soysal, H., S. Sipahioglu, D. Kolçak, and Y. Alt nok, Historical earthquake catalogue of Turkey and surrounding area (2100 B.C.–1900 A.D.), *Technical Report, TUBITAK, No. TBAG-341*, 1981.

Şengör, A. M. C. and W. S. F. Kidd, Post-collisional tectonics of the

Turkish Iranian plateau and a comparison with Tibet, *Tectonophysics*, **55**, 361–376, 1979.

Şengör, A. M. C. and Y. Y lmaz, Tethyan evolution of Turkey: A plate tectonic approach, *Tectonophysics*, **75**, 181–241, 1981.

Şengör, A. M. C., N. Görür, and F. Şaroglu, Strike-slip faulting and related basin formation in zones of tectonic escape, Strike-slip deformation, basin formation and sedimentation, *Soc. Econ. Paleontol. Mineral., Spec. Publ.*, **37**, 227–264, 1985.

Turkelli, N., E. Sandvol, E. Zor, R. Gök, T. Bekler, A. Al-Lazki, H. Karabulut, S. Kuleli, T. Eken, C. Gürbüz, S. Bayraktutan, D. Seber, and M. Barazangi, Seismogenic zones in Eastern Turkey, *Geophys. Res. Lett.*, **30**, p. 8039, doi:10.1029/2003GL018023, 2003.

Webb, T. H. and H. Kanamori, Earthquake focal mechanisms in the eastern transverse ranges and San Emigdio mountains, southern California and evidence for a regional decollement, *Bull. Seismol. Soc. Am.*, **75**(3), 737–757, 1985.

Wells, L. and J. K. Coppersmith, New empirical relationships among magnitude, rupture length, rupture width, rupture area and surface displacement, *Bull. Seismol. Soc. Am.*, **84**(4), 974–1002, 1994.

Yagi, Y, Source rupture process of the 2003 Tokachi-oki earthquake determined by joint inversion of teleseismic body wave and strong ground motion data, *Earth Planets Space*, **56**, 311–316, 2004.

Yagi, Y. and M. Kikuchi, Source rupture process of the Kocaeli, Turkey, earthquake of August 17, 1999, obtained by joint inversion of near- eld and teleseismic data, *Geophys. Res. Lett.*, **27**, 1969–1972, 2000.

Yagi, Y., T. Mikumo, J. Pacheco, and G. Reyes, Source rupture process of the Tecoma'n, Colima, Mexico earthquake of 22 January 2003, determined by joint inversion of teleseismic body-wave and near-source data, *Bull. Seismol. Soc. Am.*, **94**, 1795–1807, 2004.

Y lmaz, Y., Comparison of young associations of western and eastern Anatolia formed under compressional regime, *J. Volcanol. Geotherm. Res.*, **44**, 69–87, 1990.

Y lmaz, Y., F. Şaroglu, and Y. Güner, Initiation of the neomagmatism in East Anatolia, *Tectonophysics*, **134**, 177–199, 1987.

Y lmaz, Y., E. Yigitbaş, and Ş. C. Genç, Ophiolitic and metamorphic assemblages of southeast Anatolia and their signi cance in the geological evolution of the orogenic belt, *Tectonics*, **12**(5), 1280–1297, 1993.

Yin, A., Yu-Qi. Dang, M. Zhang, C. Xuan-Hua, and W. Michael, McRivette Cenozoic tectonic evolution of the Qaidam basin and its surrounding regions (Part 3): Structural geology, sedimentation, and regional tectonic reconstruction, *Geol. Soc. Amer. Bull.*, **120**(7–8), 847–876, doi:10.1130/B26232.1, 2008.

Yoshida, S., K. Koketsu, B. Shibazaki, T. Sagiya, T. Kato, and Y. Yoshida, Joint inversion of near- and far- eld waveforms and geodetic data for the rupture process of the 1995 Kobe earthquake, *J. Phys. Earth*, **44**, 437–454, 1996.

You-Li, C., W. Zhan-Yu, Y. Jian-Qing, H. Yong-Bing, and Z. Wen-Jun, Amounts and styles of coseismic deformation along the northern segment of surface rupture, of the 2008 Wenchuan Mw 7.9 earthquake, China, *Tectonophysics*, **491**(1–4), 35–58, 2010.

T. S. Irmak (e-mail: irmakts@kocaeli.edu.tr), B. Dogan, and A. Karakaş